

Estimation of dispersive parameters of surface wave using the generalized S transform

Roohollah Askari*, CREWES, University of Calgary.

raskari@ucalgary.ca

and

Robert J. Ferguson, CREWES, University of Calgary.

Summary

We use a mathematical model based on the generalized S transform to simultaneously estimate wavenumber, group velocity, phase velocity and frequency dependent attenuation. The group velocity is obtained from the time difference of the ridges of the transform for any frequency; the phase velocity is computed from their phase difference; and a frequency dependent attenuation is determined with respect to the proportion of the absolute amplitudes of the ridges. These parameters can be used in joint inversion for the estimation of near surface shear wave velocity. We introduce two cost functions. The first cost function is to estimate an optimum scaling factor in the generalized S transform to enable application of the method in highly dispersive media. The second cost function is to calculate a wavenumber perturbation for noisy data.

Introduction

Surface wave analysis is a well-known procedure where the phase or group velocity of dispersive surface waves is inverted to estimate shear wave velocity structure (Xia et al., 1999). The shear wave velocity is estimated from the inversion of the frequency dependent phase and group velocity. Therefore, the analysis of dispersion data to link phase and group velocity to frequency is a crucial step. Some algorithms have been developed to address these issues in different transform domains.

In this study, the generalized S transform (Pinnegar and Mansinha, 2003) is used to estimate wave propagation parameters (the wavenumber, phase velocity, group velocity and the attenuation function) for a highly dispersive medium and noisy data.

Theory

The S transform is a time-frequency spectral localization method that is similar to the short-time Fourier transform (Gabor, 1946), but, with a scalable Gaussian window which enhances time-frequency resolution. The S transform is given by Stockwell et al. (1996) as

$$S[h(\tau)](t, f) = \int_{-\infty}^{+\infty} h(\tau) \left[\frac{|f|}{\sqrt{2\pi}} e^{-\frac{f^2(\tau-t)^2}{2}} \right] e^{-j2\pi f\tau} d\tau. \quad (1)$$

where, as an operator, S transforms h, which is a function τ , into a function of frequency f and time t. A more general version of the S transform allows arbitrary variations of the Gaussian window. A version of the generalized S transform (Pinnegar and Mansinha, 2003) that has particular usefulness in our analysis is

$$S_g[h(\tau)](t, f, \sigma) = \int_{-\infty}^{+\infty} h(\tau) \frac{|f|}{\sqrt{2\pi\sigma}} e^{-\frac{f^2(\tau-t)^2}{2\sigma^2}} e^{-j2\pi f\tau} d\tau, \quad (2)$$

where the scaling factor σ controls time-frequency resolution. When σ is smaller than one, the Gaussian window is tightened in the time domain and the time resolution increases. On the other hand, for σ larger than one, the Gaussian window is expanded in the time domain and therefore the frequency resolution increases.

The wave propagation operator

Assuming that a geometrical spreading correction (cylindrical divergence) for the surface wave has been applied, if $h_1(\tau)$ is the wavelet at station 1, then the wavelet $h_2(\tau)$ recorded at station 2 is

$$H_2(f) = e^{-\lambda(f)d} e^{-j2\pi k(f)d} H_1(f), \quad (3)$$

where $\lambda(f)$ is an attenuation function, and $k(f)$ is the spatial wavenumber that controls wave propagation from station 1 to station 2. We assume that the attenuation function $\lambda(f)$ and wavenumber $k(f)$ vary slowly with respect to the effective size of the spectrum of the generalized S transform. Therefore, $\lambda(f + \alpha)$ and $k(f + \alpha)$ can be expressed as

$$\lambda(f + \alpha) = \lambda(f) + O(\alpha), \quad (4)$$

and

$$k(f + \alpha) = k(f) + \alpha k'(f) + O(\alpha^2), \quad (5)$$

where $k'(f)$ indicates a frequency derivative of $k(f)$. Upon the above approximations, we can obtain

$$S_g[h_2(\tau)] = e^{-\frac{j2\pi fd}{v_p(f)}} e^{-\lambda(f)d} S_g[h_1(\tau)] \left(t - \frac{d}{v_g(f)}, f \right), \quad (6)$$

where $S_g[h_1](t - d/v_g(f), f, \sigma)$ is the generalized S transform of h_1 shifted by $-d/v_g(f)$, and v_p and v_g are phase and group velocities respectively. Based on equation 6, any point in the time-frequency plane (t, f) of station 2 is defined from the time shifted-frequency plane $(t-d/v_g(f), f)$ of station 1 with a phase difference of $-j2\pi fd/v_p(f)$, and with an amplitude that scales $e^{-\lambda(f)d}$. Thus, the group velocity is obtained from the time difference of the ridges of the transform for any frequency; the phase velocity is computed from their phase difference; and a frequency dependent attenuation is determined with respect to the proportion of the absolute amplitudes of the ridges. To estimate the ridge of the transform, first of all, we find the time-frequency distribution of surface wave on the generalized S transform plane. Then, for every frequency, we find the maximum amplitude with respect to the time axis and consider it as the ridge of the transform for that frequency.

Figures 1a and 1b are two synthetic traces recorded at two stations. Figures 1c and 1d show the amplitude spectra of the generalized S transform of station 1 and 2 respectively. Figure 1e and Figure 1f show their phase spectra respectively. At the first step, ridges of the amplitude spectra of the transform are found (Figures 1c and 1d) at any specific frequency (here $f = 150\text{Hz}$) with respect to the time axis. Attenuation is obtained as

$$\lambda(f) = [\log(A_1(f)/A_2(f))]/d, \quad (7)$$

where A_1 and A_2 are the absolute, maximum amplitudes of the ridges of the stations respectively. Group velocity is obtained as

$$v_g(f) = d/\Delta t(f), \quad (8)$$

where $\Delta t = t_2 - t_1$ (from Figures 1c and 1d) is the time difference between two ridges. The wavenumber $k(f)$ is computed from

$$k(f) = -\Delta\phi(f)/2\pi d, \quad (9)$$

where $\Delta\phi$ is the phase difference between two ridges (Figures 1e and 1f). Finally the phase velocity is calculated using

$$v_p(f) = f/k(f). \quad (10)$$

In cases where the medium is highly dispersive, and a signal has a wide band of frequencies, there is a high uncertainty in the estimated amplitude and phase spectra at high frequencies due to low frequency resolution (Mallat, 1999). However, the generalized S transform improves frequency resolution of high frequencies when we select a larger value of σ . Thus, we are able to estimate propagation parameters of surface wave for highly dispersive and attenuating media. Figure 2 shows a wavelet signal dispersed in a relatively highly dispersive medium with a dominant wavelet frequency of 125 Hz. As seen in

Figures 3a-3d the wavenumber, phase velocity and attenuation obtained using scaling factor $\sigma=20$ are poorly estimated for higher frequencies. This error implies that the phase and amplitude spectra of high frequencies are poorly estimated. We expect to improve these results by choosing larger values for σ for this example. The hashed lines in Figure 3 show the estimated propagation operators based on $\sigma=100$. The estimated wavenumber, phase velocity and attenuation function are now improved, as expected.

Since, in time, resolution decreases with σ , there is a tradeoff in resolution for wavenumber and attenuation with the resolution for group velocity. Therefore, σ may not be chosen too large. So that we might automate the process of selecting an optimal value of σ , we use the following cost function

$$E(\sigma) = \left\| S_{g_i}(t, f) - S_{g_r} \left(t - \frac{D_i}{v_g(f)}, f \right) e^{-\lambda_{\sigma}(f)D_i} e^{-i2\pi k_{\sigma}(f)D_i} \right\|^2, \quad (11)$$

where $\lambda_{\sigma}(f)$ is the calculated attenuation and $k_{\sigma}(f)$ is the calculated wavenumber based on a specific value of σ respectively, S_{g_i} is the generalized S transform of the i th geophone, S_{g_r} is the generalized S transform of a reference geophone which could be the first geophone of a record, and D_i is the distance between the reference and the i th geophone. Figures 4a and 4b show two dispersed synthetic data sets with different dispersivities. The second data set is more dispersed in comparison with the first one. Figures 4c and 4d show the cost function for both data sets respectively. The cost function for the first data converts to zero at $\sigma = 5$, and for the second data converts to zero at $\sigma = 22$. It can be concluded that for highly dispersive media, a higher value of σ should be chosen. In other words, σ is a function of the dispersivity of a medium.

Synthetic data example

Figure 5 shows a synthetic record where the geophones are irregularly spaced. The average distance between two adjacent geophones, however, is set to be 200m. The signal to noise ratio is 5, and the noise is white Gaussian. Figure 6 shows the estimated wave number, phase velocity, group velocity and attenuation. The estimated wavenumber and phase velocity are not consistent with the theoretical values. The wavenumber of the model (km) can be expressed as approximately equal to the estimated wavenumber (k_e) plus a perturbation according to

$$k_m \approx k_e + \varepsilon. \quad (12)$$

Equation 12 can be explained by the effect of noise at low frequency components where the signal to noise ratio is small. At those frequencies, initial values of phase (φ_0) are highly affected by noise, hence, any phase difference between two geophones is not directly proportional to the wavenumber. The group velocity and the attenuation function are better estimated around 22.5 Hz where the signal to noise ratio is large. The group velocity is more highly distorted around zero frequency due to the small signal to noise ratio and the low time resolution at low frequencies.

The problem can be solved using the least squares solution by finding an appropriate value for the wavenumber perturbation ε . The assumption is $|\varepsilon| \ll 1$. The cost function to be minimized is

$$E(\varepsilon) = \left\| S_{g_i}(t, f) - S_{g_r} \left(t - \frac{D_i}{v_g(f)}, f \right) e^{-\lambda(f)D_i} e^{-i2\pi k_e(f)D_i} e^{-i2\pi \varepsilon D_i} \right\|^2, \quad (13)$$

where S_{g_i} is the generalized S transform of the i th geophone, S_{g_r} is the generalized S transform of a reference geophone. In this study the first geophone is assigned as the reference, and D_i is the distance between the reference and the i^{th} geophone. The cost function is highly non-linear and has lots of local minima, so it is impossible to solve it using some gradient methods such as Steepest Descent or Conjugate Gradient. In this paper, Simulated Annealing (Beatty et al., 2002) is used to find an optimum value for epsilon. The optimum value of $\varepsilon = 1.89 \times 10^{-3}$ is obtained. Figure 6 shows the wavenumber and the phase velocity corrected based on the computed value for epsilon. The corrected wavenumber and corrected phase velocity match very well with the theoretical value.

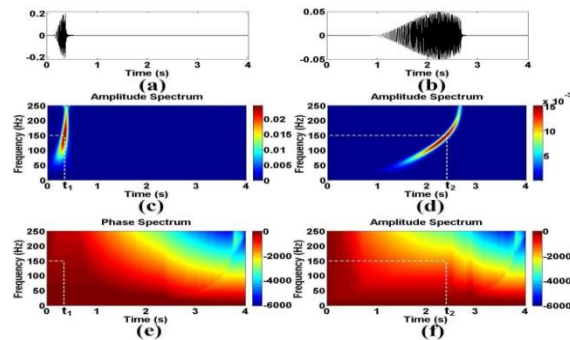


Figure 1: (a) and (b) two synthetic traces. (c) and (d) the amplitude spectra of (a) and (b) respectively. (e) and (f) the phase spectra of (a) and (b) respectively.

Real data example

The real data used in this study was acquired from the foothills of the Canadian Rocky Mountains, southern Alberta, at the University of Calgary's Rothney Astrophysical/Geophysical Observatory. The source is an IVI Envirovibe (18,000 lb) sweeping from 10 to 250 Hz with an eleven second listen time and a four times vertical stack. The receivers are 10 Hz 3-C geophones. We use the vertical component for ground roll dispersion analysis. Figure 7 shows the real data consisting of dispersive ground roll with a sampling frequency of 1000 Hz and a sampling distance one meter. Figure 8 shows the estimated propagation parameters obtained from the generalized S transform. The estimated phase, group and attenuation are in a reasonable range for near-surface materials. We note here that the calculated attenuation is comparable to some near surface study results for these frequency ranges (e.g. Xia et al., 2002, Kulesh et al., 2005, Holschneider et al., 2005). There are some small fluctuations on the calculated attenuation which can be referred to the effect of noise. We see this effect (small fluctuations on the calculated attenuation) on the synthetic data example too. The attenuation at 30Hz is smaller than at 15 Hz. It can be concluded that there is a near surface layer with less attenuation than deeper layers. The estimated group velocity at the frequency ranges from 15Hz to 35Hz differs significantly from the phase velocity. The estimated group velocity is less than the phase velocity. The trend of the group velocity is also different from that of the phase velocity. Other authors report similar group velocity ranges and trends for near surface studies (e.g. Kulesh et al., 2005 and Holschneider et al., 2005).

Conclusions

The generalized S transform provides frequency-dependent resolution while maintaining a direct relationship with the Fourier spectrum. Using this property, the wavenumber and phase velocity, group velocity and frequency dependent attenuation function are obtained directly from the phase and amplitude spectrum of the transform based on its ridges. The advantage of the generalized S transform over the S transform lies in the fact that it manipulates time-frequency resolution in the S domain using a scaling factor. Therefore, results can be improved, especially for a highly dispersive and dissipative medium. According to the results, for a highly dispersive medium, a larger value of the scaling factor must be chosen. However, we are usually limited to choosing an appropriate scaling factor due to overlapping time-frequency spectra of different modes for specific values of the scaling factor. We introduce a cost function to estimate an optimum value for a given scaling factor. Experimentally we find that the estimated wavenumber is perturbed for noisy data when signal to noise ratio is small at low frequencies. As a remedy, we estimate wavenumber perturbation by minimizing a cost function using Simulated Annealing.

Acknowledgements

The authors wish to thank the sponsors of the CREWES, as well as the NSERC, for their support of this work. We also thank Dr. Rolf Maier and Faranak Mahmoudian for editing this paper.

References

Beatty, K. D.R. Schmitt, and M. Sacchi, 2002, Simulated annealing inversion of multimode Rayleigh wave dispersion curves for geological structure: *Geophys. J. Int.*, 151, 622-671

Gabor, D., 1946, Theory of communication: *J. Inst. Elect. Eng.*, 93, 429-457.

Holschneider, M., Diallo, M. S., Kulesh, M., Ohrnberger, M., Lück, E., and Scherbaum, F., 2005, Characterization of dispersive surface waves using continuous wavelet transforms: *Geophys. J. Int.*, 163, 463-478.

Kulesh, M., Holschneider, M., Diallo, M. S., Xie, Q., and Scherbaum, F., 2005, Modeling of wave dispersion using continuous wavelet transforms: *Pure and Applied Geophysics*, 162, 843-855.

Mallat, S., 1999, A wavelet tour of signal processing: Academic Press, London, UK.

Pinnegar, C. R., and Mansinha, L. 2003, The Bi-Gaussian S-transform: *SIAM J. SCI. COMPUT.*, 24, 1678-1692.

Stockwell, R. G., Mansinha, L., and Lowe, R. P., 1996, Localization of the complex spectrum: The S transform: *IEEE Transactions on Signal Processing*, 44, 998-1001.

Xia, J., Miller, R.D., and Park, C.B., 1999, Estimation of near-surface shear-wave velocity by inversion of Rayleigh waves: *Geophysics*, 64, 691-700.

Xia, J., Miller, R. D., Park, C. B., Hunter, J. A., Harris, J. B., and Ivanov J, 2002, Comparing shear wave velocity profiles inverted from multichannel surface wave with borehole measurements: *Soil Dynamics and Earthquake Engineering*, 22, 181-190.

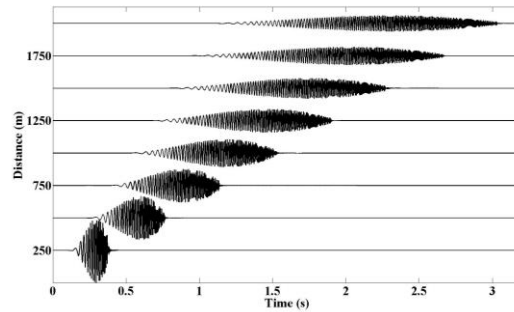


Figure 2: A wavelet signal dispersed in a relatively high dispersive medium recorded at different geophones.

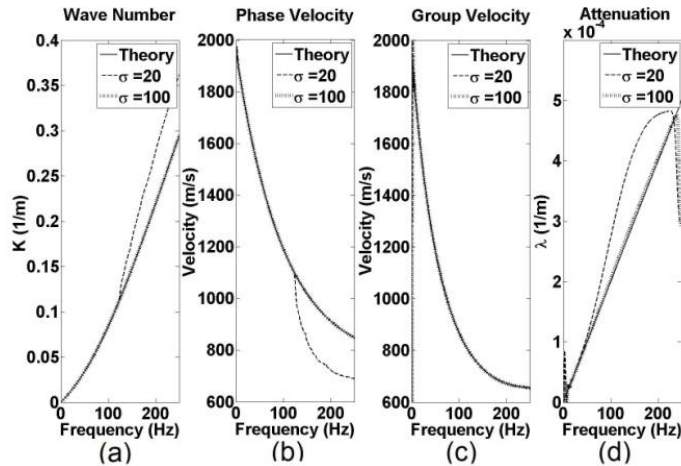


Figure 3: The estimated wavenumber, phase and group velocities and attenuation functions based on the scaling factors $\sigma=20$ (dashed lines) and $\sigma=100$ (hashed lines).

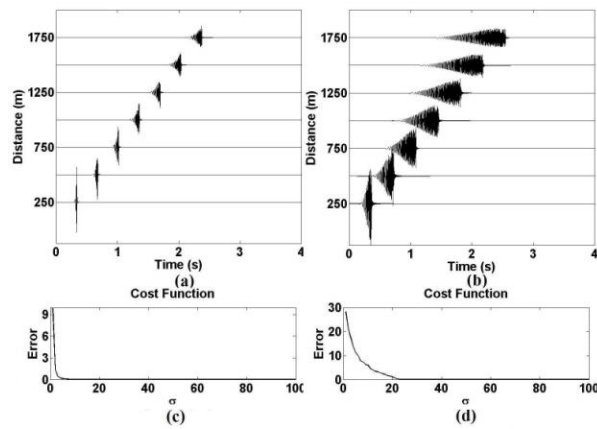


Figure 4: (a) and (b) two different dispersed data sets. (c) and (d) the cost functions for (a) and (b) respectively.

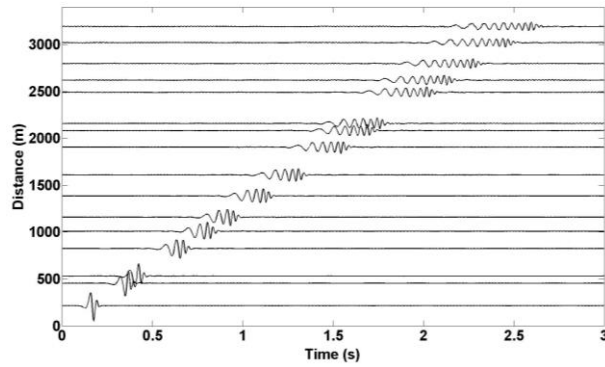


Figure 5: A noisy synthetic seismic record with a dispersive Ricker wavelet.

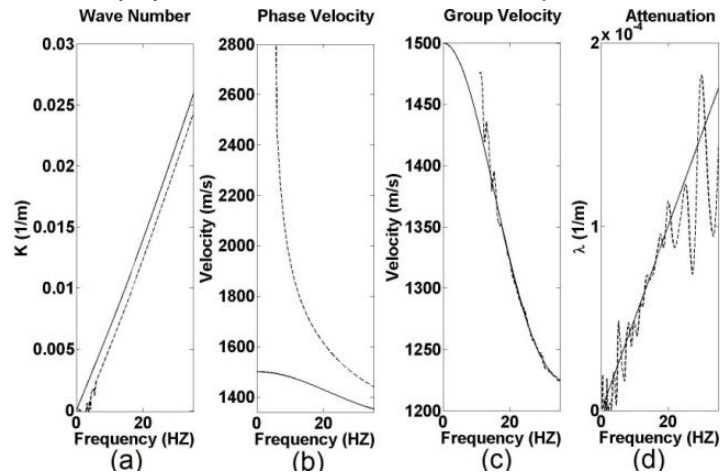


Figure 6: The estimated wavenumber, phase and group velocities and attenuation functions (dashed lines). The solid lines correspond to the theoretical values.

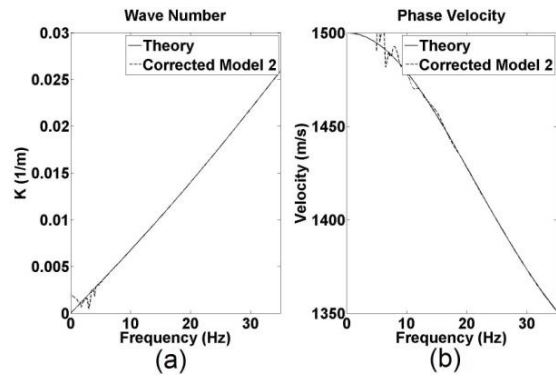


Fig. 7: (a) The wavenumber. And (b) phase velocity corrected based on computed optimum value for epsilon.

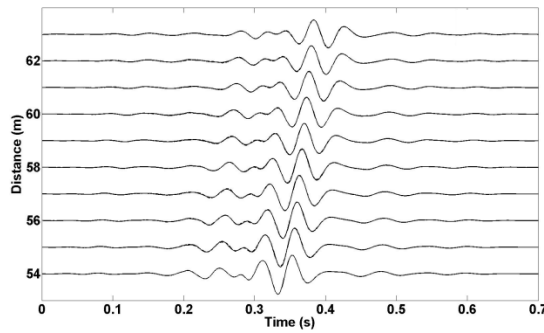


Figure 8: a real data.

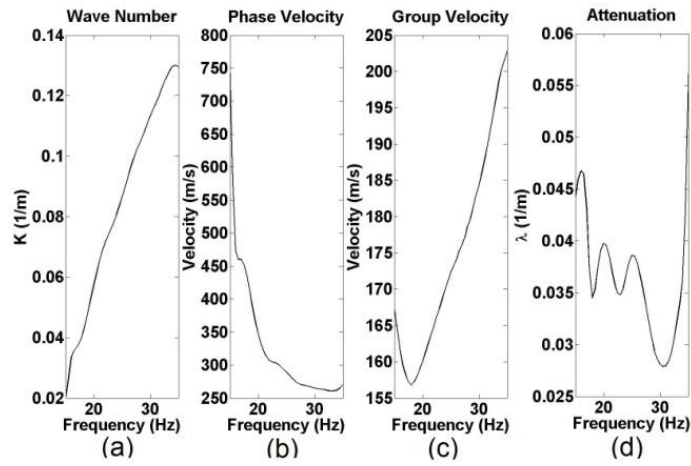


Figure 9: Estimated propagation model parameters of the real data. (a) The wavenumber. (b) The phase velocity. (c) The group velocity. (d) The attenuation function.